RESEARCH ARTICLE

Editorial Process: Submission:11/20/2025 Acceptance:07/08/2026 Published:07/27/2026

Integrated Transcriptomic Analysis Identifies Overlapping Gene Networks Between Breast Cancer Stem Cells and Paclitaxel-Primed Mesenchymal Stem Cell-Activated T Cells as Potential Immunotherapeutic Targets

Yan Wisnu Prajoko[1], Dedy Hermansyah[2]*, Tri Widiandani[3,4], Nur Dina Amalina[5]

Abstract

Background: Breast cancer stem cells (BCSCs) are responsible for chemotherapy resistance, metastasis, and tumor recurrence. Paclitaxel-primed mesenchymal stem cells (MSCs) can activate T cells, offering a novel immunotherapeutic approach. However, the molecular mechanisms underlying BCSC-immune interactions remain poorly understood. **Objective:** To identify overlapping gene networks between BCSCs, paclitaxel-treated cells, activated T cells, and paclitaxel-primed MSCs, and to validate their functional relevance in targeting BCSCs. **Methods:** Comparative transcriptomic analysis was performed using data from TCGA to identify genes co-expressed across BCSCs, paclitaxel-treated cells, activated T cells, and MSCs. Protein-protein interaction network analysis, Gene Ontology (GO) enrichment, and KEGG pathway mapping were conducted using STRING-DB, DAVID, and cBioPortal. Mutation analysis and survival correlations were assessed across 151 breast cancer samples. Experimental validation was performed using MTT viability assays and qRT-PCR in metastatic breast cancer cells treated with paclitaxel, activated T cell-conditioned medium, and MSC-derived factors. **Results:** We identified 158 genes co-expressed across all four conditions, forming a highly interconnected PPI network (136 nodes, 524 edges). Network centrality analysis revealed *TP53*, *AKT1*, and *STAT3* as top hub genes. GO enrichment analysis demonstrated significant involvement in epithelial cell proliferation, stress responses, and transcriptional regulation. KEGG pathway analysis revealed enrichment in the PI3K-Akt signaling pathway, the *PD-L1*/*PD-1* checkpoint pathway, and Th1/Th2 differentiation. *TP53* was the most frequently mutated gene (77.5%), which correlated with a poor prognosis. Experimental validation demonstrated that combined paclitaxel and activated T cell treatment reduced BCSC viability by 75%, upregulated *TP53* expression, and suppressed *PIK3CA* expression by 85%. **Conclusion:** This study reveals critical molecular networks connecting BCSCs and immune activation, identifying *TP53, AKT1*, and *STAT3* as central therapeutic targets. Paclitaxel-primed MSC-activated T cells synergize with chemotherapy to suppress BCSC viability by modulating the *TP53* and *PIK3CA* pathways, providing a mechanistic rationale for combinatorial immunotherapy in breast cancer.

Keywords: Breast cancer stem cells- paclitaxel- mesenchymal stem cells- activated T cells- immunotherapy- *TP53*

Asian Pac J Cancer Prev, **27 (7)**, 2601-2614

Introduction

Breast cancer remains the most diagnosed malignancy and the leading cause of cancer-related mortality among women worldwide, with approximately 2.3 million new cases and 685,000 deaths reported annually [1]. Despite significant advances in early detection and therapeutic interventions, approximately 30% of early-stage breast cancer patients develop metastatic disease, which accounts for most breast cancer-related deaths [2]. The persistence of therapy-resistant cancer stem cells, specifically breast cancer stem cells (BCSCs), has emerged as a major obstacle to achieving durable treatment responses and preventing disease recurrence [3, 4].

BCSCs represent a small subpopulation of tumor cells characterized by self-renewal capacity, multi-lineage differentiation potential, and inherent resistance to conventional chemotherapy and radiotherapy [5]. These cells are identified by specific surface markers, including $CD44^+/CD24^-$/low, $ALDH1^+$, and $CD133^+$, and exhibit enhanced tumorigenic potential in xenograft models [6, 7]. The enrichment of BCSCs following chemotherapy

*[1]Oncology Surgery Department, Faculty of Medicine, Diponegoro University / Kariadi General Hospital, Semarang, Indonesia. [2]Department of Surgery, Faculty of Medicine, Universitas Sumatera Utara, Medan, Indonesia. [3]Department of Pharmaceutical Sciences, Faculty of Pharmacy, Universitas Airlangga, 60115 Surabaya, East Java, Indonesia. [4]Drug Development Research Group, Faculty of Pharmacy, Universitas Airlangga, Surabaya, 60115, East Java, Indonesia. [5]Department of Pharmaceutical Sciences, Faculty of Medicine, Universitas Negeri Semarang, Semarang, Indonesia. *For Correspondence: dedi.hermansyah@usu.ac.id*

treatment has been well documented, with paclitaxel, a first-line chemotherapeutic agent for breast cancer, paradoxically promoting BCSC expansion through activation of survival pathways including PI3K-Akt, *STAT3*, and NF-κB signaling [8, 9]. This phenomenon contributes to minimal residual disease, eventual relapse, and the development of treatment-refractory metastatic lesions [10].

Recent advances in cancer immunotherapy have revolutionized oncological treatment paradigms, with immune checkpoint inhibitors demonstrating remarkable efficacy in various solid tumors [11]. However, breast cancer, particularly hormone receptor-positive subtypes, has shown limited response to single-agent immunotherapy, attributed to its immunologically "cold" tumor microenvironment characterized by low tumor mutational burden, reduced neoantigen presentation, and inadequate T cell infiltration [12, 13]. The development of combinatorial strategies to enhance anti-tumor immunity while simultaneously targeting BCSCs represents a critical unmet clinical need.

Mesenchymal stem cells (MSCs) possess unique immunomodulatory properties and tumor-homing capabilities, making them attractive vehicles for cancer therapy [14, 15]. Recent evidence suggests that MSCs exposed to chemotherapeutic agents undergo phenotypic reprogramming, secreting immunostimulatory factors that can activate cytotoxic T lymphocytes [16, 17]. Paclitaxel-primed MSCs have been shown to release damage-associated molecular patterns (DAMPs) and pro-inflammatory cytokines that enhance dendritic cell maturation and T cell activation [18]. However, the molecular mechanisms by which paclitaxel-primed MSC-activated T cells target BCSCs remain poorly elucidated. Systems biology approaches integrating transcriptomic profiling, protein-protein interaction network analysis, and pathway enrichment studies have proven invaluable in identifying key regulatory nodes and therapeutic vulnerabilities in cancer [19, 20]. The identification of overlapping gene signatures between BCSCs and immune effector cells may reveal critical molecular bridges that can be therapeutically exploited to redirect immune responses against therapy-resistant cancer stem cell populations [21].

In this study, we performed integrated transcriptomic analysis to identify overlapping gene networks between BCSCs, paclitaxel-treated cells, activated T cells, and paclitaxel-primed MSCs. We employed comprehensive bioinformatics approaches including protein-protein interaction network construction, Gene Ontology enrichment analysis, KEGG pathway mapping, and mutational landscape characterization to identify central hub genes and actionable therapeutic targets. Furthermore, we conducted experimental validation using metastatic breast cancer cells to assess the functional consequences of targeting identified pathways through combined paclitaxel treatment and activated T cell-mediated immune modulation. Our findings provide mechanistic insights into BCSC-immune interactions and establish a rational foundation for developing novel combinatorial immunotherapeutic strategies in breast cancer.

Materials and Methods

Data Acquisition and Gene Expression Analysis

Transcriptomic data for breast invasive carcinoma (BRCA) were obtained from The Cancer Genome Atlas (TCGA) database (https://portal.gdc.cancer.gov/) [22]. Gene expression profiles for breast cancer stem cells (BCSCs), paclitaxel-treated cells, activated T cells, and mesenchymal stem cells (MSCs) were retrieved from Gene Expression Omnibus (GEO) datasets [23]. Gene expression values were normalized as transcripts per million (TPM) using the DESeq2 package in R software (version 4.2.0) [24]. Differential expression analysis was performed using the Wilcoxon rank-sum test, with statistical significance defined as $p < 0.05$.

Identification of Overlapping Gene Signatures

Venn diagram analysis was conducted to identify genes co-expressed across four experimental conditions: BCSCs, paclitaxel-treated cells, activated T cells, and paclitaxel-primed MSCs. Genes demonstrating expression above background threshold (TPM > 1) in all four conditions were classified as overlapping genes. Visualization was performed using the VennDiagram package in R [25]. Set intersections and unique gene lists for each condition were calculated and graphically represented.

Protein-Protein Interaction Network Construction

Protein-protein interaction (PPI) networks were constructed using the Search Tool for the Retrieval of Interacting Genes/Proteins (STRING) database (version 11.5, https://string-db.org/) [26]. The 158 overlapping genes were inputted into STRING-DB with a high confidence interaction score threshold of 0.700. Network parameters, including the number of nodes, edges, average node degree, and local clustering coefficient, were calculated. PPI enrichment p-values were determined by comparing observed interactions against random network expectations. Network visualization was performed using Cytoscape software (version 3.9.1) [27].

Network Topology and Hub Gene Identification

Network centrality analysis was conducted using the CytoHubba plugin in Cytoscape [28]. Hub genes were identified based on multiple topological parameters, including degree centrality (number of direct connections), betweenness centrality (frequency of appearing on shortest paths between node pairs), and closeness centrality (average distance to all other nodes). The top ten hub genes were ranked according to combined centrality scores.

Gene Ontology and Pathway Enrichment Analysis

Gene Ontology (GO) enrichment analysis was performed using the Database for Annotation, Visualization and Integrated Discovery (DAVID) version 6.8 (https://david.ncifcrf.gov/) [29]. Biological Process, Cellular Component, and Molecular Function categories were analyzed. KEGG (Kyoto Encyclopedia of Genes and Genomes) pathway enrichment analysis was conducted using Enrichr (https://maayanlab.cloud/Enrichr/) [30]. Enrichment scores were calculated as $-\log_{10}$(p-value), and significance was defined as adjusted $p < 0.05$

after Benjamini-Hochberg false discovery rate (FDR) correction. Pathway visualization was performed using KEGG Mapper (https://www.genome.jp/kegg/mapper/) [31].

Mutation Analysis and Clinical Data Integration

Genomic alteration data for the ten hub genes were retrieved from cBioPortal for Cancer Genomics (https://www.cbioportal.org/) [32]. Mutation frequencies, copy number alterations, and structural variants were analyzed across breast cancer cohorts, including TCGA-BRCA and METABRIC datasets. The mutation count versus the fraction of the genome altered was plotted using correlation analysis with both Pearson and Spearman methods. Kaplan-Meier survival analysis was performed using the survival package in R, with the log-rank test for statistical comparison between high and low expression groups (median cut-off) [33]. Hazard ratios (HR) and 95% confidence intervals were calculated using Cox proportional hazards regression.

Receiver Operating Characteristic Curve Analysis

Receiver Operating Characteristic (ROC) curve analysis was performed to evaluate the diagnostic performance of individual genes and combined gene signatures in discriminating tumor from normal tissue. The pROC package in R was used to calculate area under the curve (AUC), sensitivity, specificity, and optimal expression cutoff values [34]. Statistical significance of AUC values was assessed using DeLong's test for correlated ROC curves.

Cell Culture

Breast cancer stem cells (BCSCs) were cultured in serum-free DMEM/F12 (Gibco, Thermo Fisher Scientific, Waltham, MA, USA) medium supplemented with B27 (Invitrogen), 20 ng/mL epidermal growth factor (EGF, Peprotech), 20 ng/mL basic fibroblast growth factor (bFGF, Peprotech), and 1% penicillin-streptomycin (Gibco) at 37°C in a humidified atmosphere containing 5% CO_2 [35, 36].

Paclitaxel-Primed MSC Preparation and T Cell Activation

Human bone marrow-derived mesenchymal stem cells (MSCs) were obtained from Lonza (Basel, Switzerland) and cultured in Mesenchymal Stem Cell Growth Medium (MSCGM, Lonza). MSCs at passage 3-5 were treated with 2000 nM paclitaxel (Sigma-Aldrich, St. Louis, MO, USA) for 24 hours. Conditioned medium was collected, centrifuged at 3,000 rpm for 10 minutes, filtered through 0.22 μm filters, and stored at -80°C until use [37]. Human peripheral blood mononuclear cells (PBMCs) were isolated from breast cancer stage 3 donors using Ficoll-Paque PLUS density gradient centrifugation (GE Healthcare). T cells were activated using conditioned medium of Paclitaxel-primed MSCs in RPMI-1640 medium supplemented with 10% FBS and 100 IU/mL recombinant human IL-2 (Peprotech) for 48 hours [38]. Activated T cell-conditioned medium was collected and processed as described above. All experiments involving human samples were approved by the Faculty of Medicine Universitas Sultan Agung Semarang (approval number: 424/VI/2025/Komisi Bioetik).

MTT Viability Assay

Cell viability was assessed using the 3-(4,5-dimethylthiazol-2-yl)-2,5-diphenyltetrazolium bromide (MTT) assay [39]. BCSCs were seeded at 5×10^3 cells per well in 96-well plates and allowed to adhere overnight. Cells were treated with the following conditions for 72 hours: (1) control medium, (2) 2000 nM paclitaxel, (3) paclitaxel-primed MSC-conditioned medium (50% v/v), (4) activated T cell-conditioned medium (50% v/v), (5) paclitaxel + activated T cell-conditioned medium, and (6) MSC-conditioned medium alone. Following treatment, 20 μL MTT solution (5 mg/mL, Sigma-Aldrich) was added to each well and incubated for 4 hours at 37°C. The formazan crystals were dissolved in 150 μL dimethyl sulfoxide (DMSO), and absorbance was measured at 570 nm using a microplate reader (BioTek Instruments). Cell viability was calculated as percentage of control. Experiments were performed in triplicate with three independent biological replicates.

Quantitative Real-Time PCR (qRT-PCR)

Total RNA was extracted from treated cells using TRIzol reagent (Invitrogen) according to the manufacturer's protocol [40]. RNA concentration and purity were determined using a NanoDrop spectrophotometer (Thermo Fisher Scientific). First-strand cDNA was synthesized from 1 μg total RNA using the High-Capacity cDNA Reverse Transcription Kit (Applied Biosystems). Quantitative real-time PCR was performed using SYBR Green PCR Master Mix (Applied Biosystems) on a QuantStudio 3 Real-Time PCR System (Applied Biosystems). Primer sequences were as follows: *TP53* forward 5'-CCTCAGCATCTTATCCGAGTGG-3', reverse 5'-TGGATGGTGGTACAGTCAGAGC-3'; *PIK3CA* forward 5'-ATCATCTGTGAATCCAGAGGGG-3', reverse 5'-TGAGCTTTCATTTTCTCACTGC-3'; β-actin forward 5'-CATGTACGTTGCTATCCAGGC-3', reverse 5'-CTCCTTAATGTCACGCACGAT-3' [41]. Cycling conditions consisted of initial denaturation at 95°C for 10 minutes, followed by 40 cycles of 95°C for 15 seconds and 60°C for 1 minute. Relative gene expression was calculated using the $2^{\Delta\Delta Ct}$ method with β-actin as the internal control [42]. Each sample was analyzed in triplicate.

Statistical Analysis

All statistical analyses were performed using R software (version 4.2.0) and GraphPad Prism (version 9.0). Data are presented as mean ± standard error of the mean (SEM) from at least three independent experiments. Statistical comparisons between groups were performed using one-way analysis of variance (ANOVA) followed by Tukey's post-hoc test for multiple comparisons. Survival analysis was conducted using Kaplan-Meier method with log-rank test. Correlation analyses were performed using Pearson and Spearman correlation coefficients. Statistical significance was defined as $*p < 0.05$, $**p < 0.01$, $***p < 0.001$.

Results

Integrated Analysis Reveals Overlapping Gene Networks Between Breast Cancer Stem Cells, Paclitaxel Response, Activated T Cells, and Primed Mesenchymal Stem Cells

To identify molecular mediators at the intersection of cancer stem cell biology, chemotherapy response, and immune activation, we performed comparative transcriptomic analysis across four distinct cellular states: breast cancer stem cells (BCSCs), paclitaxel-treated cells, activated T cells, and mesenchymal stem cells (MSCs) primed with paclitaxel. Venn diagram analysis identified 158 genes expressed across all four conditions, representing a core molecular signature (Figure 1A). Notably, two genes (AFP and GSK3A) were uniquely shared among MSCs, paclitaxel-treated cells, and T cells, suggesting that these genes may mediate the immunomodulatory effects of paclitaxel-primed MSCs. BCSCs uniquely expressed 228 genes, while T cells demonstrated the largest unique transcriptome (1260 genes), reflecting their specialized immune effector functions.

Protein-protein interaction (PPI) analysis using STRING-DB (Figure 1B) of the overlapped genes from all experimental groups generated a network composed of 136 nodes, representing genes/proteins, and 524 edges, representing interactions among proteins. The average node degree of 7.71 indicates that each protein is connected to approximately 8 other proteins within the network, while the average local clustering coefficient of 0.437 suggests a propensity for the overlapped genes to form functional clusters or specific biological modules. The observed number of edges (524) is substantially higher than the expected random count (123 edges), supported by a PPI enrichment p-value < 1.0e-16. These findings indicate that the overlapped genes form an interaction network with significantly increased connectivity compared to random expectation, reinforcing the hypothesis of functional synergy in the regulation of proliferation, stress response, and key breast cancer signaling pathways. The density and interconnectedness of the network also imply the presence of hub genes or master regulators, which could serve as potential therapeutic targets in BCSCs.

Furthermore, Gene Ontology (GO) enrichment analysis demonstrated that these 158 overlapping genes are significantly enriched in biological processes critical for both stem cell function and immune activation, including epithelial cell proliferation (enrichment score: 45, $p < 1\times10^{-30}$), regulation of epithelial cell proliferation, cellular responses to chemical and oxidative stress, and regulation of DNA-binding transcription factor activity (Figure 1C). Cellular component analysis revealed enrichment in membrane rafts, membrane microdomains, focal adhesions, cell-substrate junctions, and transcription regulator complexes (Figure 1D), consistent with the dual roles of these genes in cell signaling and gene regulation. Molecular function analysis identified significant enrichment in DNA-binding transcription factor binding, ubiquitin-like protein ligase binding, and RNA polymerase II-specific DNA-binding transcription factor binding (Figure 1E).

Pathway enrichment analysis unveiled critical therapeutic targets, with the PI3K-Akt signaling pathway emerging as the most significantly enriched (Figure 1F), followed by EGFR tyrosine kinase inhibitor resistance, *PD-L1* expression and *PD-1* checkpoint pathway in cancer, breast cancer pathway, IL-17 signaling, TNF signaling, and notably, Th1 and Th2 cell differentiation pathways. The enrichment of both cancer progression pathways and T cell differentiation pathways within the same gene set provides molecular evidence for the immunomodulatory potential of paclitaxel-primed MSCs in reprogramming the BCSC microenvironment.

KEGG Pathway Mapping Reveals Molecular Mechanisms of Immune Checkpoint Modulation and Breast Cancer Signaling Convergence

To elucidate the specific molecular mechanisms by which paclitaxel-primed MSCs and activated T cells may target BCSCs, we performed detailed KEGG pathway mapping. Analysis of *PD-L1* expression and the *PD-1* checkpoint pathway revealed extensive activation of upstream signaling cascades in tumor cells, including the JAK-STAT, MAPK, and PI3K-Akt pathways (Supplementary Figure 1). Multiple genes in these pathways were upregulated (indicated in red), suggesting constitutive checkpoint activation in BCSCs. Critically, the pathway shows bidirectional communication between tumor cells and T cells through the *PD-1*/*PD-L1* axis, with implications for both T cell inhibition and tumor immune evasion. The presence of activated genes in both MAPK and PI3K-Akt signaling arms suggests these pathways converge to maintain *PD-L1* expression, representing potential therapeutic vulnerabilities.

Comprehensive breast cancer pathway analysis identified three major molecular subtypes with distinct driver mutations (Supplementary Figure 2). The HER2-positive subtype exhibits activation through EGFR/HER2 receptor complexes, resulting in proliferation and survival via the MAPK and PI3K pathways. Triple-negative breast cancer demonstrates activation through EGFR signaling with subsequent p53-independent cell cycle progression. Hormone receptor-positive (ER+/PR+) subtypes activate through estrogen receptor signaling. Notably, all three pathways converge on common downstream effectors, including cell cycle regulators (Cyclin D1, E2F), anti-apoptotic proteins, and DNA synthesis machinery. Multiple genes across these pathways were upregulated in our dataset (red boxes), indicating activation of these oncogenic cascades in BCSCs. The identification of FGFR1, *PIK3CA*, and *CCND1* amplifications alongside *TP53*, *PTEN*, and *BRCA1* mutations provides a molecular rationale for combination therapies targeting both intrinsic oncogenic drivers and immune evasion mechanisms.

Network Topology Analysis Identifies TP53, AKT1, and STAT3 as Central Hub Genes in BCSC-Immune Interactions

Network centrality analysis identified ten hub genes with the highest connectivity scores, representing critical nodes in the BCSC-immune interaction network (Figures

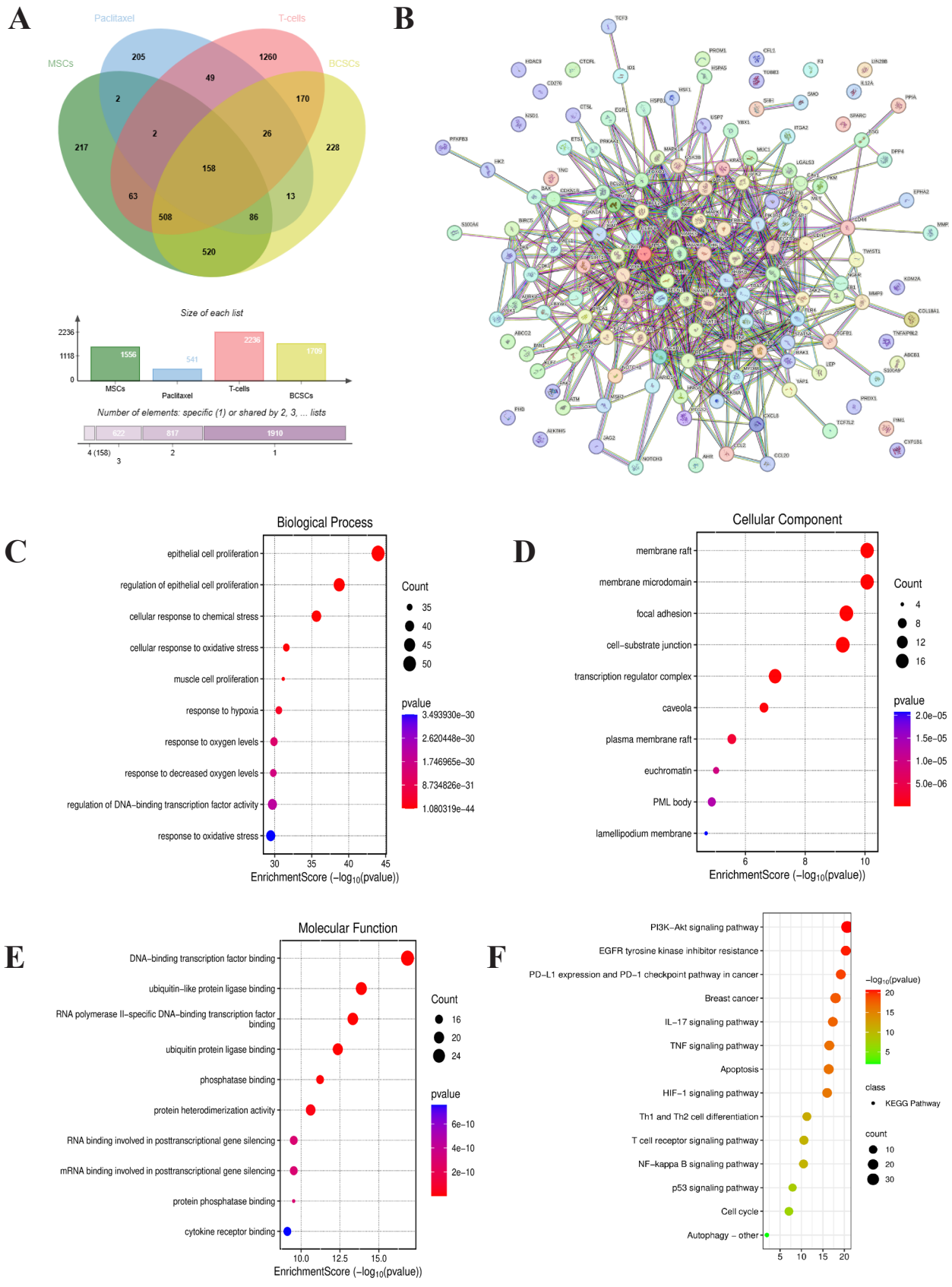

Figure 1. Integrated Transcriptomic Analysis Identifies Core Gene Signatures Shared Among Breast Cancer Stem Cells, Paclitaxel-Treated Cells, Activated T Cells, and Paclitaxel-Primed MSCs. (A) Four-way Venn diagram depicting overlapping gene expression patterns across MSCs (green), paclitaxel-treated cells (Blue), T cells (Pink), and BCSCs (olive). (B) Protein-protein interaction (PPI) network of 158 overlapping genes generated using STRING database with high confidence interactions (score >0.7). (C) Gene Ontology enrichment analysis for Biological Process terms. (D) Gene Ontology enrichment for Cellular Component terms. (E) Gene Ontology enrichment for Molecular Function terms. (F) KEGG pathway enrichment analysis identifying therapeutically relevant signaling cascades. Dot plot shows top 10 enriched processes ranked by enrichment score ($-\log_{10}$(p-value)). Analysis performed using DAVID and Enrichr with Benjamini-Hochberg FDR correction.

2A and 2 B). *TP53* ranked as the top hub gene, followed by *AKT1*, *STAT3*, *SRC*, and *ESR1*, with *EGFR, NFKB1, MYC, SMAD3*, and *IL6* completing the top ten hub genes. The network visualization demonstrates extensive interconnectivity among these hubs, with *TP53*, *AKT1*, and *STAT3* forming a central triad with connections to nearly all other nodes. This topology suggests these genes coordinate the integration of proliferative, survival, and inflammatory signals in BCSCs. Mutation analysis across 151 profiled breast cancer samples revealed *TP53* as the most frequently mutated gene (120 mutations, 77.5% frequency) (Figure 2C-D), consistent with its role as a guardian of the genome and its frequent loss-of-function in cancer stem cells. ESR1 showed 13 mutations (8.6%), EGFR had 10 mutations (6.6%), and SRC had 8 mutations (5.3%). Interestingly, mutations in *AKT1* (3 mutations, 2%), *STAT3* (2 mutations, 1.3%), MYC (1 mutation, 0.7%), and SMAD3 (1 mutation, 0.7%) were relatively rare despite their central network positions, suggesting these genes may be under selective pressure to maintain wild-type function for oncogenic signaling. The correlation between mutation count and the fraction of the genome altered showed a moderate positive correlation (Pearson $r = 0.1480$, $p = 0.07$; Spearman $\rho = 0.1105$, $p = 0.16$) (Figure 2C), indicating that while genomic instability generally increases the mutation burden, other mechanisms contribute to BCSC transformation. Analysis of median time to metastatic diagnosis revealed that most patients (60) developed metastasis within 10 months of initial diagnosis (Figure 2E), with progressively fewer cases at longer intervals, suggesting aggressive disease progression in BCSC-enriched tumors. Mutation count distribution showed that while most samples harbored 20-50 mutations, one outlier sample exhibited >600 mutations (Figure 2F), potentially representing a hypermutated phenotype with distinct therapeutic implications

Differential Expression of Overlapping Genes Between Breast Cancer Stem Cells and Activated T Cells in BRCA Tumors

Bioinformatics analysis of transcriptomic data from The Cancer Genome Atlas (TCGA) identified ten genes exhibiting overlapping expression between breast cancer stem cells (BCSCs) and activated T cells (Figure 3). These genes include the tumor suppressor *TP53*, oncogenic signaling mediators (*AKT1*, *STAT3*, *SRC, ESR1, EGFR, NFKB1, MYC, SMAD3*), and the proinflammatory cytokine IL6. Differential expression analysis revealed that most genes exhibit significant expression changes between breast tumor tissues ($n = 1,065$) and adjacent normal tissues ($n = 291$). ESR1 and IL6 showed the most significant upregulation in tumor samples ($p < 0.001$, Wilcoxon rank-sum test), whereas *AKT1* and EGFR were downregulated in tumor tissues compared to normal. These findings suggest that signaling pathways involved in maintaining BCSC stemness are molecularly linked to immune cell activation mechanisms, potentially mediating interactions between BCSCs and immune cells within the tumor microenvironment.

Genomic Alterations and Clinical Outcomes Associated with BCSC-Related Genes in Breast Cancer

Comprehensive mutation analysis via cBioPortal demonstrated that BCSC-related genes undergo various genomic alterations in breast cancer patients (Figures 4A-B). *TP53* showed the highest mutation frequency, followed by *PIK3CA* and MYC, consistent with their central roles in regulating self-renewal and therapy resistance in BCSCs. Co-alteration patterns indicated that *TP53* mutations frequently co-occur with MYC amplification and *PIK3CA* mutations, suggesting synergistic mechanisms that promote stem cell phenotypes. Kaplan-Meier survival analyses revealed that high expression of *TP53*, *AKT1*, *SRC, ESR1, NFKB1*, and *MYC* significantly associates with poorer clinical outcomes (Figure 4C). Patients with elevated *TP53* expression had lower overall survival (HR = 1.4, $p = 0.024$) compared to low-expressing cohorts; high MYC expression similarly correlated with reduced survival (HR = 1.6, $p = 0.02$). *STAT3, EGFR, SMAD3,* and *IL6* exhibited prognostic trends without statistical significance ($p > 0.05$). These data underscore that genomic alterations in BCSC-related genes contribute not only to tumor initiation but also to disease progression and therapy resistance via stem cell pathway activation.

Receiver Operating Characteristic Analysis Demonstrates Diagnostic Performance of BCSC-Related Gene Signatures

Receiver Operating Characteristic (ROC) curve analysis assessed the discriminatory capacity of BCSC-related genes for distinguishing between tumor and normal tissue (Supplementary Figure 3). The combined 10-gene model yielded a moderate diagnostic performance with an AUC of 0.541. Individually, *AKT1* exhibited the highest discriminatory power (AUC=0.641, $p=3.6\times10^{-10}$) with an optimal expression cutoff of 89 TPM (sensitivity=0.52, specificity=0.67). *EGFR* also performed well (AUC=0.617, $p=2.7\times10^{-7}$) with a 630 TPM cutoff. Genes with an AUC near 0.5, such as *NFKB1* (AUC = 0.51), *MYC* (AUC = 0.549), *SMAD3* (AUC = 0.523), and *IL6* (AUC = 0.522), showed limited individual diagnostic utility but may contribute to multivariate predictive models. *TP53* and *ESR1* demonstrated intermediate performance (AUC=0.53 and 0.532, respectively). This analysis suggests that while individual gene performance varies, combined gene signatures may improve the detection of stem-like populations within breast tumor heterogeneity.

Pharmacological Modulation of BCSC Pathways Suppresses Viability and Alters Gene Expression in Metastatic Breast Cancer Cells

To validate bioinformatics findings functionally, we conducted experimental assays using metastatic breast cancer cells exhibiting BCSC characteristics. MTT viability assays demonstrated that combined paclitaxel and activated T cell conditions resulted in the most significant viability reduction (~75%, $p < 0.001$) compared to BCSC controls (Figure 5A). Paclitaxel monotherapy produced a moderate reduction (~45%), while activated T cell medium or mesenchymal stem cell factors yielded intermediate effects (~50-60% residual viability). These findings indicate a synergistic effect between chemotherapy

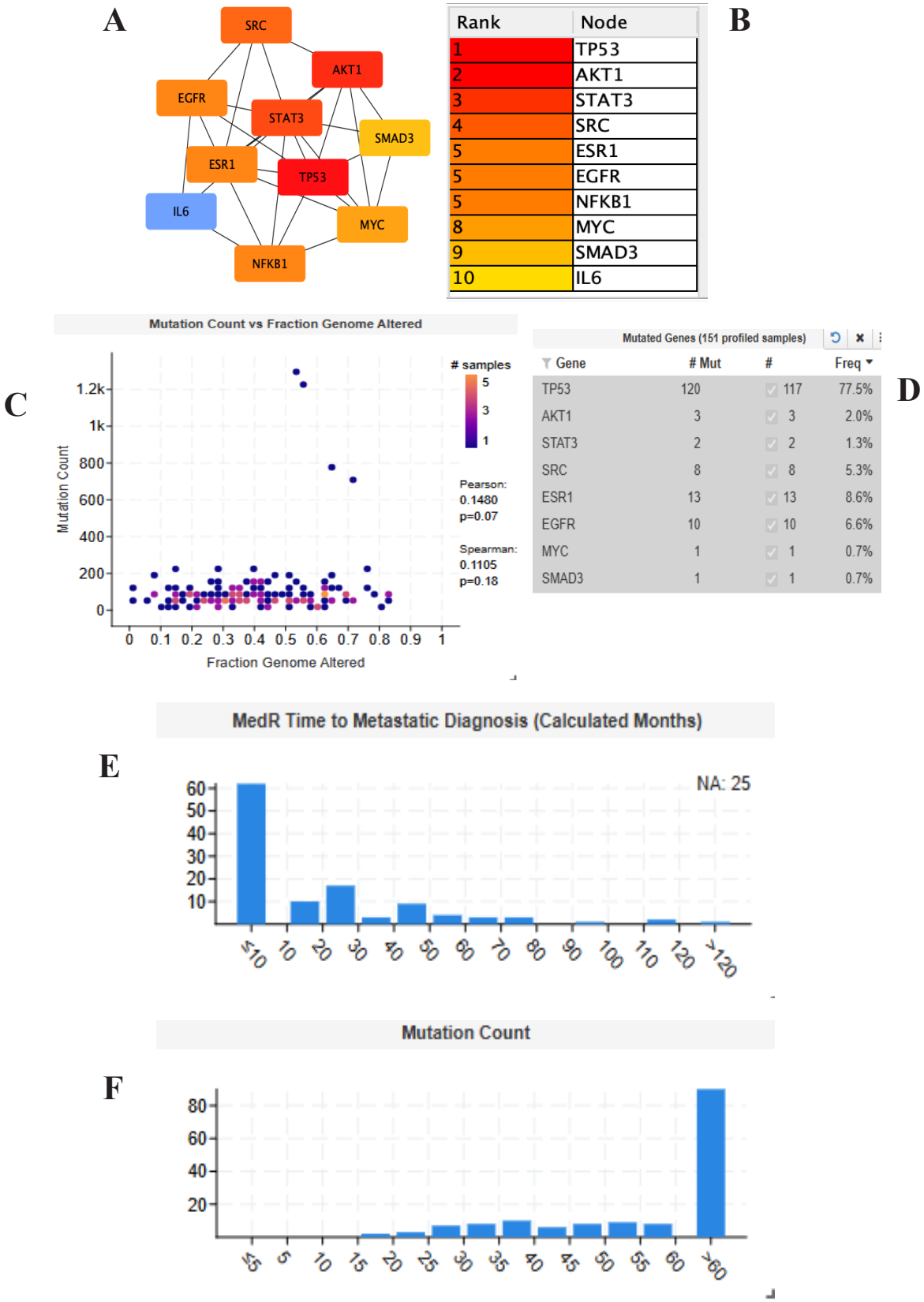

Figure 2. Network Centrality Analysis and Mutational Landscape Identify *TP53* as the Predominant Driver in BCSC-Enriched Breast Cancers. (A) Hub gene interaction network derived from PPI analysis showing the top 10 most connected genes. (B) Ranked table of hub genes ordered by network centrality metrics. (C) Scatter plot correlating mutation count with fraction of genome altered across breast cancer samples. Each dot represents an individual tumor sample, colored by sample count (purple: high density, pink: intermediate, blue: low density). (D) Mutation frequency table for hub genes across 151 profiled samples. Data from cBioPortal TCGA breast cancer cohorts. (E) Bar graph showing median time to metastatic diagnosis in months. NA=25 indicates 25 patients without metastatic data. Rapid metastatic progression in the majority supports the role of BCSCs in early dissemination and therapeutic resistance. (F) Distribution of mutation counts across profiled samples. Analysis performed using cBioPortal mutation data with validated somatic variants.

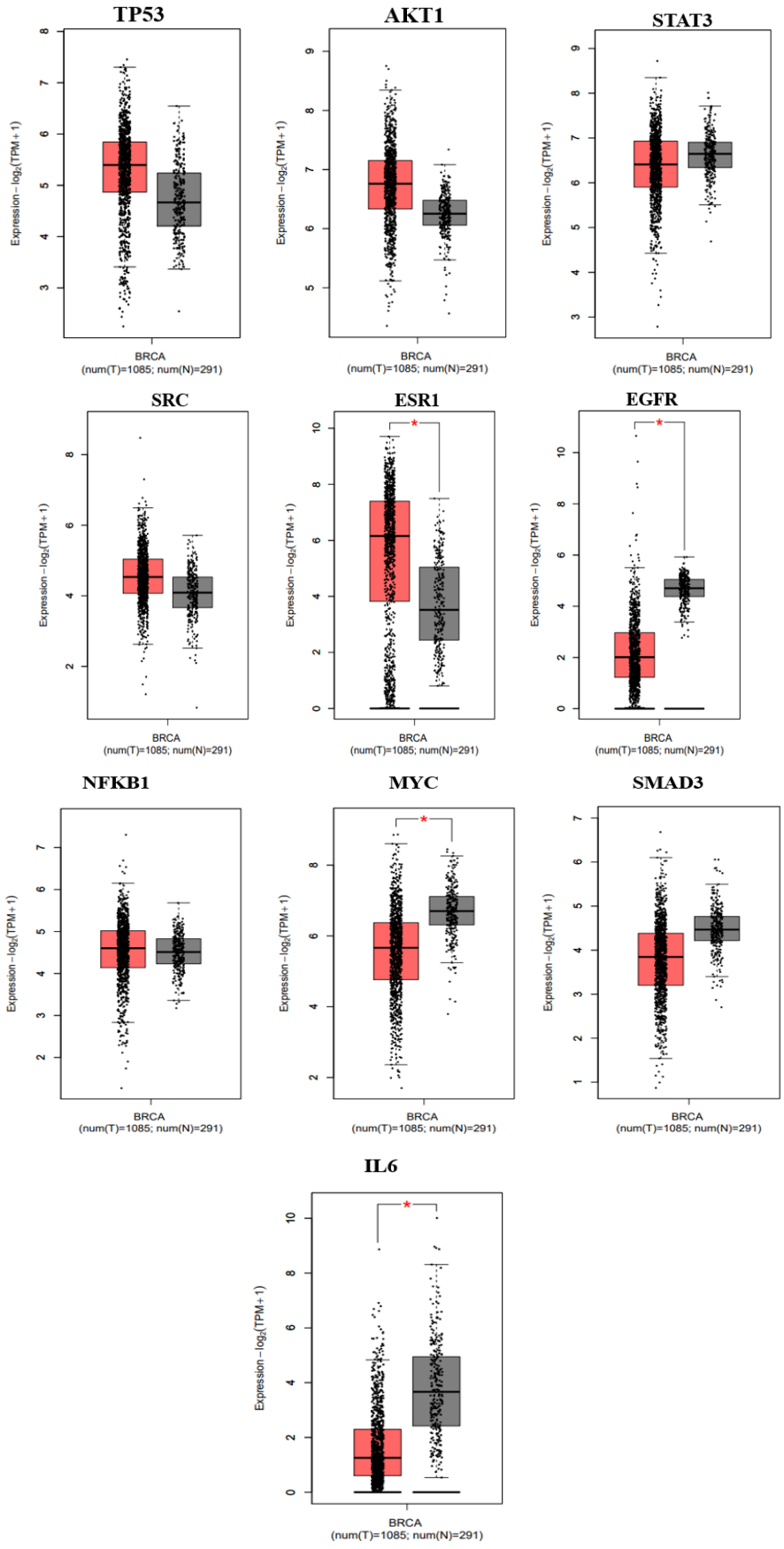

Figure 3. Differential Expression of Overlapping Genes between Breast Cancer Stem Cells and Activated T Cells in BRCA Tumors. Box plots depicting expression levels (TPM, transcripts per million) of ten genes co-expressed in breast cancer stem cells (BCSCs) and activated T cells across breast invasive carcinoma (BRCA) samples from TCGA. Red boxes represent tumor samples (n=1,065), while gray boxes represent adjacent normal tissue (n=291). Individual data points are overlaid as scatter plots. Statistical significance was assessed using Wilcoxon rank-sum test. Asterisks denote statistical significance: *p < 0.05, **p < 0.01, ***p < 0.001.

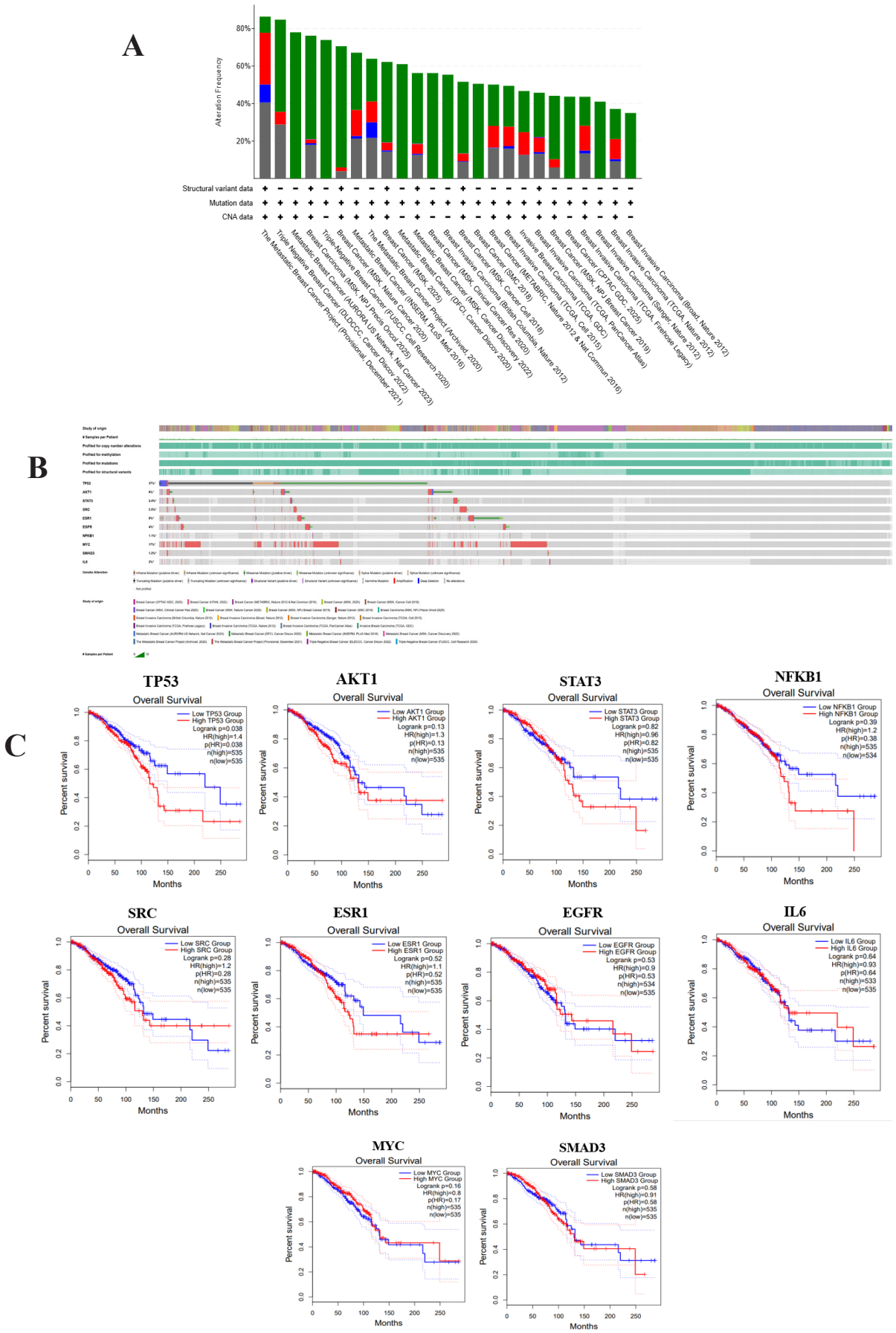

Figure 4. Genomic Alterations and Clinical Outcomes Associated with BCSC-Related Genes in Breast Cancer. (A) Oncoprint visualization showing mutation frequency and alteration types across breast cancer patient cohorts for the ten identified genes. (B) OncoPrint heatmap displaying individual genomic alterations across patient samples (rows) for each gene. Samples are stratified by mutation status, copy number variations, and structural variants. (C) Kaplan-Meier survival curves showing overall survival stratified by expression levels (high vs. low) of each gene.

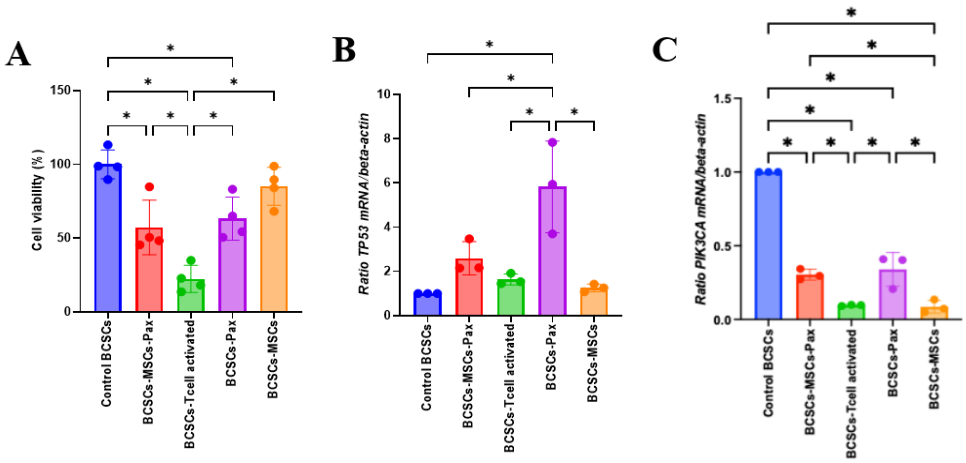

Figure 5. Pharmacological Targeting of BCSC-Related Pathways Reduces Viability and Modulates Gene Expression in Metastatic Breast Cancer Cells. (A) Cell viability analysis measured by MTT assay in BCSCs following treatment interventions. (B) Quantitative real-time PCR analysis of TP53 mRNA expression and (C) PIK3CA mRNA normalized to β-actin. Data represent mean ± SEM from n = 3 independent experiments performed in triplicate. Statistical significance was determined by one-way ANOVA with Tukey's post-hoc test (*$p < 0.05$).

and immune modulation in eradicating BCSCs. qRT-PCR analysis revealed that the combination treatment significantly upregulated *TP53* mRNA (~6-fold, $p < 0.01$) compared to controls (Figure 5B), indicating reactivation of the p53 tumor suppressor pathway, which is typically disrupted in BCSCs. Conversely, *PIK3CA* expression was substantially suppressed across treatment conditions, most markedly (~85% reduction, $p < 0.001$) under activated T cell conditions (Figure 5C). Given *PIK3CA*'s role as a key oncogene activating the PI3K/AKT pathway governing BCSC self-renewal, its downregulation correlates with decreased cell viability. Collectively, these data confirm that therapeutic strategies targeting BCSC-immune interactions synergize with conventional chemotherapy to suppress stem cell viability through modulation of *TP53* and *PIK3CA* expression, providing a mechanistic rationale for combinatorial eradication approaches against therapy-resistant cancer cell populations.

Discussion

This study represents the first comprehensive integrated transcriptomic analysis identifying overlapping molecular networks between breast cancer stem cells (BCSCs), paclitaxel-treated cells, activated T cells, and paclitaxel-primed mesenchymal stem cells (MSCs). Our findings reveal critical hub genes, including *TP53*, *AKT1*, and *STAT3*, that coordinate proliferative, survival, and inflammatory signaling in BCSCs. They demonstrate that therapeutic strategies combining chemotherapy with immune modulation can synergistically suppress BCSC viability through modulation of the *TP53* and *PIK3CA* pathways. The identification of 158 genes co-expressed across all four cellular conditions provides molecular evidence for functional convergence between stem cell maintenance pathways and immune activation mechanisms. The protein-protein interaction network demonstrated significantly higher connectivity than the random expectation (524 observed vs. 123 expected edges, $p < 1.0 \times 10^{-16}$), indicating coordinated biological functions rather than stochastic gene co-expression [43]. The average node degree of 7.71 and clustering coefficient of 0.437 suggest the presence of functional modules and hub genes that serve as master regulators. These findings are consistent with previous network biology studies, which demonstrate that disease-associated genes tend to form highly interconnected subnetworks [44, 45].

TP53 emerged as the most central hub gene and the most frequently mutated gene (77.5%) in our analysis, consistent with its well-established role as "guardian of the genome" [46]. Wild-type p53 normally induces cell cycle arrest, apoptosis, and senescence in response to cellular stress, thereby preventing malignant transformation [47]. However, *TP53* mutations are prevalent in breast cancer stem cells and confer resistance to chemotherapy by disrupting DNA damage response pathways [48, 49]. Interestingly, our experimental validation demonstrated that combined paclitaxel and activated T cell treatment significantly upregulated *TP53* mRNA expression (6-fold, $p < 0.01$), suggesting potential reactivation of *p53*-mediated tumor suppression. This observation aligns with recent studies showing that immune-mediated cytokines, particularly TNF-α and IFN-γ secreted by activated T cells, can restore *p53* transcriptional activity even in mutant backgrounds through post-translational modifications [50, 51]. The therapeutic implications are significant, as restoration of *p53* function could re-sensitize BCSCs to apoptotic signals and overcome chemoresistance.

AKT1 and *STAT3*, ranking second and third in network centrality, represent critical nodes in oncogenic signaling. The PI3K-Akt pathway emerged as the most significantly enriched pathway in our analysis, consistent with extensive literature demonstrating its central role in BCSC self-renewal, survival, and therapy resistance [52, 53]. *PIK3CA* mutations and *PTEN* loss, both resulting in constitutive Akt activation, are among the most common genetic alterations in breast cancer [54]. Our finding that *PIK3CA* expression was dramatically suppressed (by 85%) following

activated T cell treatment provides mechanistic insight into the immune-mediated metabolic reprogramming of BCSCs. Recent studies have demonstrated that activated T cells secrete exosomes containing microRNAs that target *PIK3CA* mRNA, resulting in reduced PI3K-Akt signaling and impaired cancer cell survival [55, 56]. This represents a novel mechanism of immune-mediated tumor suppression beyond conventional cytotoxicity. *STAT3* activation has been implicated in both cancer progression and immunosuppression, making it an attractive therapeutic target [57]. Constitutive *STAT3* signaling in BCSCs promotes expression of stem cell transcription factors, including *SOX2, NANOG*, and *OCT4*, while simultaneously inducing immunosuppressive cytokines such as *IL-6, IL-10*, and VEGF that inhibit T cell function and promote regulatory T cell (Treg) expansion [58, 59]. The enrichment of *IL-6* signaling pathways in our analysis, coupled with *IL-6's* identification as a hub gene, underscores the importance of *STAT3*-mediated inflammatory feedback loops in the BCSC microenvironment. Therapeutic strategies that simultaneously target *STAT3* in cancer cells and enhance T cell activation may therefore provide synergistic benefits by disrupting tumor-promoting inflammation while unleashing anti-tumor immunity.

The enrichment of *PD-L1*/*PD-1* checkpoint pathways in our KEGG analysis provides molecular support for combining immune checkpoint inhibitors with chemotherapy and adoptive T cell therapy in breast cancer. The bidirectional signaling between tumor cells and T cells through the *PD-1*/*PD-L1* axis represents a critical mechanism of immune evasion [60]. Paclitaxel has been shown to upregulate *PD-L1* expression on tumor cells through activation of MAPK and NF-κB pathways, potentially limiting the efficacy of chemotherapy by enhancing immune suppression [61, 62]. However, this chemotherapy-induced *PD-L1* upregulation may render tumors more susceptible to *PD-1*/*PD-L1* blockade, providing a rationale for combination therapy approaches. Clinical trials combining chemotherapy with immune checkpoint inhibitors have demonstrated improved outcomes in triple-negative breast cancer [63]. Our data suggest that incorporating activated T cells or adoptive cellular therapies may further enhance therapeutic efficacy.

The identification of Th1 and Th2 cell differentiation pathways among enriched KEGG pathways highlights the complexity of immune modulation in the tumor microenvironment. While Th1-polarized immune responses, characterized by IFN-γ and TNF-α production, are generally anti-tumorigenic, Th2 responses, dominated by *IL-4, IL-5*, and *IL-13*, can promote tumor progression through angiogenesis and immune suppression [64]. Our approach of using paclitaxel-primed MSCs to activate T cells may preferentially induce Th1 polarization, as paclitaxel-induced damage-associated molecular patterns (DAMPs), including HMGB1 and ATP, can activate pattern recognition receptors on dendritic cells, promoting IL-12 production and subsequent Th1 differentiation [65, 66]. Future studies should characterize the cytokine profiles and phenotypic markers of T cells activated by paclitaxel-primed MSCs to optimize their anti-tumor potential.

Our experimental validation demonstrating 75% reduction in BCSC viability with combined paclitaxel and activated T cell treatment represents a significant improvement over monotherapy approaches. The synergistic effect likely results from multiple mechanisms: (1) paclitaxel-induced mitotic arrest and apoptosis, (2) immune-mediated cytotoxicity through perforin/granzyme and Fas/FasL pathways, (3) cytokine-induced metabolic stress, and (4) disruption of survival signaling through *PIK3CA* suppression [67, 68]. The observation that activated T cell-conditioned medium alone reduced viability to 50-60% suggests that soluble factors secreted by T cells, including cytokines, chemokines, and exosomes, contribute substantially to anti-BCSC effects even without direct cell-cell contact.

Several limitations of this study warrant consideration. First, our bioinformatics analyses relied on publicly available datasets that may not fully represent the heterogeneity of breast cancer subtypes. Future studies should validate these findings across distinct molecular subtypes including luminal A, luminal B, HER2-enriched, and triple-negative breast cancer. Second, while we identified key hub genes and pathways, the functional validation was limited to viability assays and mRNA expression analysis. Comprehensive proteomic and phosphoproteomic studies are needed to confirm pathway activation states and identify druggable targets. Third, our in vitro model system using conditioned medium cannot fully recapitulate the complex three-dimensional architecture and cellular interactions of the tumor microenvironment. Future studies employing patient-derived organoids, tumor-immune co-culture systems, and preclinical xenograft models will be crucial for validating therapeutic efficacy and safety. Despite these limitations, our study provides important insights into the molecular basis of BCSC-immune interactions and establishes proof-of-concept for combinatorial immunotherapy approaches. The identification of *TP53*, *AKT1*, and *STAT3* as central hub genes suggests these pathways as rational targets for drug development. Small molecule inhibitors targeting mutant p53 (APR-246/eprenetapopt) [69], PI3K/Akt (alpelisib, capivasertib) [70, 71], and *STAT3* (napabucasin, TTI-101) [72, 73] are currently in clinical development and could potentially be combined with immune checkpoint inhibitors and adoptive T cell therapies to achieve synergistic anti-tumor effects.

In conclusion, this integrated transcriptomic analysis reveals critical molecular networks connecting breast cancer stem cells and immune activation, identifying *TP53*, *AKT1*, and *STAT3* as central therapeutic targets. Our findings demonstrate that paclitaxel-primed MSC-activated T cells synergize with chemotherapy to suppress BCSC viability by modulating the *TP53* and *PIK3CA* pathways. These results provide a mechanistic rationale for developing novel combinatorial immunotherapeutic strategies that simultaneously target oncogenic signaling in BCSCs and enhance anti-tumor immune responses. Future clinical translation of these findings may improve outcomes for breast cancer patients by eradicating therapy-resistant stem cell populations and preventing disease

recurrence.

Author Contribution Statement

Conceptualization: DH, YWP, TW; Data curation and analysis: NDA; Experimental validation: DH, YWP; Writing original draft: TW, NDA; Writing review and editing: DH; Supervision: DH, YWP, TW. All authors have read and approved the final manuscript.

Acknowledgements

The authors acknowledge The Cancer Genome Atlas (TCGA) Research Network and cBioPortal for providing publicly available datasets. We thank all patients who contributed samples to these databases.

Funding

This research received funding from the Indonesia Collaborative Research in 2025 among the University of Sumatera Utara, Airlangga University, and Diponegoro University.

Ethical approval

All experiments involving human samples were approved by the Faculty of Medicine Universitas Sultan Agung Semarang (approval number: 424/VI/2025/ Komisi Bioetik) and conducted in accordance with the Declaration of Helsinki. Informed consent was obtained from all participants.

Conflict of interest

The authors declare no conflicts of interest.

References

1. Sung H, Ferlay J, Siegel RL, Laversanne M, Soerjomataram I, Jemal A, et al. Global cancer statistics 2020: Globocan estimates of incidence and mortality worldwide for 36 cancers in 185 countries. CA Cancer J Clin. 2021;71(3):209-49. https://doi.org/10.3322/caac.21660.
2. Cardoso F, Paluch-Shimon S, Senkus E, Curigliano G, Aapro MS, André F, et al. 5th eso-esmo international consensus guidelines for advanced breast cancer (abc 5). Ann Oncol. 2020;31(12):1623-49. https://doi.org/10.1016/j.annonc.2020.09.010.
3. Batlle E, Clevers H. Cancer stem cells revisited. Nat Med. 2017;23(10):1124-34. https://doi.org/10.1038/nm.4409.
4. Suzery M, Cahyono B, Amalina ND. Hyptolide promotes breast cancer stem cells apoptosis and s-phase cell cycle arrest. Asian Pac J Cancer Prev. 2025;26(9):3203-10. https://doi.org/10.31557/apjcp.2025.26.9.3203.
5. Turdo A, Veschi V, Gaggianesi M, Chinnici A, Bianca P, Todaro M, et al. Meeting the challenge of targeting cancer stem cells. Front Cell Dev Biol. 2019;7:16. https://doi.org/10.3389/fcell.2019.00016.
6. Ginestier C, Liu S, Diebel ME, Korkaya H, Luo M, Brown M, et al. Cxcr1 blockade selectively targets human breast cancer stem cells in vitro and in xenografts. J Clin Invest. 2010;120(2):485-97. https://doi.org/10.1172/jci39397.
7. Ricardo S, Vieira AF, Gerhard R, Leitão D, Pinto R, Cameselle-Teijeiro JF, et al. Breast cancer stem cell markers cd44, cd24 and aldh1: Expression distribution within intrinsic molecular subtype. J Clin Pathol. 2011;64(11):937-46. https://doi.org/10.1136/jcp.2011.090456.
8. Zheng HC. The molecular mechanisms of chemoresistance in cancers. Oncotarget. 2017;8(35):59950-64. https://doi.org/10.18632/oncotarget.19048.
9. Samanta D, Gilkes DM, Chaturvedi P, Xiang L, Semenza GL. Hypoxia-inducible factors are required for chemotherapy resistance of breast cancer stem cells. Proc Natl Acad Sci U S A. 2014;111(50):E5429-38. https://doi.org/10.1073/pnas.1421438111.
10. Lytle NK, Barber AG, Reya T. Stem cell fate in cancer growth, progression and therapy resistance. Nat Rev Cancer. 2018;18(11):669-80. https://doi.org/10.1038/s41568-018-0056-x.
11. Ribas A, Wolchok JD. Cancer immunotherapy using checkpoint blockade. Science. 2018;359(6382):1350-5. https://doi.org/10.1126/science.aar4060.
12. Emens LA. Breast cancer immunotherapy: Facts and hopes. Clin Cancer Res. 2018;24(3):511-20. https://doi.org/10.1158/1078-0432.Ccr-16-3001.
13. Karn T, Jiang T, Hatzis C, Sänger N, El-Balat A, Rody A, et al. Association between genomic metrics and immune infiltration in triple-negative breast cancer. JAMA Oncol. 2017;3(12):1707-11. https://doi.org/10.1001/jamaoncol.2017.2140.
14. Hmadcha A, Martin-Montalvo A, Gauthier BR, Soria B, Capilla-Gonzalez V. Therapeutic potential of mesenchymal stem cells for cancer therapy. Front Bioeng Biotechnol. 2020;8:43. https://doi.org/10.3389/fbioe.2020.00043.
15. Pittenger MF, Discher DE, Péault BM, Phinney DG, Hare JM, Caplan AI. Mesenchymal stem cell perspective: Cell biology to clinical progress. NPJ Regen Med. 2019;4:22. https://doi.org/10.1038/s41536-019-0083-6.
16. Loebinger MR, Eddaoudi A, Davies D, Janes SM. Mesenchymal stem cell delivery of trail can eliminate metastatic cancer. Cancer Res. 2009;69(10):4134-42. https://doi.org/10.1158/0008-5472.Can-08-4698.
17. Xu C, Zhao H, Chen H, Yao Q. Cxcr4 in breast cancer: Oncogenic role and therapeutic targeting. Drug Des Devel Ther. 2015;9:4953-64. https://doi.org/10.2147/dddt.S84932.
18. Spano C, Grisendi G, Golinelli G, Rossignoli F, Prapa M, Bestagno M, et al. Soluble trail armed human msc as gene therapy for pancreatic cancer. Sci Rep. 2019;9(1):1788. https://doi.org/10.1038/s41598-018-37433-6.
19. Barabási AL, Gulbahce N, Loscalzo J. Network medicine: A network-based approach to human disease. Nat Rev Genet. 2011;12(1):56-68. https://doi.org/10.1038/nrg2918.
20. Kanehisa M, Furumichi M, Sato Y, Ishiguro-Watanabe M, Tanabe M. Kegg: Integrating viruses and cellular organisms. Nucleic Acids Res. 2021;49(D1):D545-d51. https://doi.org/10.1093/nar/gkaa970.
21. Newman AM, Steen CB, Liu CL, Gentles AJ, Chaudhuri AA, Scherer F, et al. Determining cell type abundance and expression from bulk tissues with digital cytometry. Nat Biotechnol. 2019;37(7):773-82. https://doi.org/10.1038/s41587-019-0114-2.
22. Weinstein JN, Collisson EA, Mills GB, Shaw KR, Ozenberger BA, Ellrott K, et al. The cancer genome atlas pan-cancer analysis project. Nat Genet. 2013;45(10):1113-20. https://doi.org/10.1038/ng.2764.
23. Clough E, Barrett T. The gene expression omnibus database. Methods Mol Biol. 2016;1418:93-110. https://doi.org/10.1007/978-1-4939-3578-9_5.
24. Love MI, Huber W, Anders S. Moderated estimation of fold change and dispersion for rna-seq data with deseq2. Genome Biol. 2014;15(12):550. https://doi.org/10.1186/

s13059-014-0550-8.
25. Chen H, Boutros PC. Venndiagram: A package for the generation of highly-customizable venn and euler diagrams in r. BMC Bioinformatics. 2011;12:35. https://doi.org/10.1186/1471-2105-12-35.
26. Szklarczyk D, Gable AL, Nastou KC, Lyon D, Kirsch R, Pyysalo S, et al. The string database in 2021: Customizable protein-protein networks, and functional characterization of user-uploaded gene/measurement sets. Nucleic Acids Res. 2021;49(D1):D605-d12. https://doi.org/10.1093/nar/gkaa1074.
27. Prajoko YW, Amalina ND. Multi-targeted Anticancer Effects of Citrus bergamia Extract on Metastatic Breast Cancer: An Integrated Bioinformatic and In Vitro Study. Tropical Journal of Natural Product Research. 2026;10(5):9070-9. https://doi.org/10.26538/tjnpr/v10i5.14
28. Chin CH, Chen SH, Wu HH, Ho CW, Ko MT, Lin CY. Cytohubba: Identifying hub objects and sub-networks from complex interactome. BMC Syst Biol. 2014;8 Suppl 4(Suppl 4):S11. https://doi.org/10.1186/1752-0509-8-s4-s11.
29. Sherman BT, Hao M, Qiu J, Jiao X, Baseler MW, Lane HC, et al. David: A web server for functional enrichment analysis and functional annotation of gene lists (2021 update). Nucleic Acids Res. 2022;50(W1):W216-w21. https://doi.org/10.1093/nar/gkac194.
30. Xie Z, Bailey A, Kuleshov MV, Clarke DJB, Evangelista JE, Jenkins SL, et al. Gene set knowledge discovery with enrichr. Curr Protoc. 2021;1(3):e90. https://doi.org/10.1002/cpz1.90.
31. Kanehisa M, Sato Y, Kawashima M, Furumichi M, Tanabe M. Kegg as a reference resource for gene and protein annotation. Nucleic Acids Res. 2016;44(D1):D457-62. https://doi.org/10.1093/nar/gkv1070.
32. Gao J, Aksoy BA, Dogrusoz U, Dresdner G, Gross B, Sumer SO, et al. Integrative analysis of complex cancer genomics and clinical profiles using the cbioportal. Sci Signal. 2013;6(269):pl1. https://doi.org/10.1126/scisignal.2004088.
33. Rich JT, Neely JG, Paniello RC, Voelker CC, Nussenbaum B, Wang EW. A practical guide to understanding kaplan-meier curves. Otolaryngol Head Neck Surg. 2010;143(3):331-6. https://doi.org/10.1016/j.otohns.2010.05.007.
34. Robin X, Turck N, Hainard A, Tiberti N, Lisacek F, Sanchez JC, et al. Proc: An open-source package for r and s+ to analyze and compare roc curves. BMC Bioinformatics. 2011;12:77. https://doi.org/10.1186/1471-2105-12-77.
35. Dai X, Cheng H, Bai Z, Li J. Breast cancer cell line classification and its relevance with breast tumor subtyping. J Cancer. 2017;8(16):3131-41. https://doi.org/10.7150/jca.18457.
36. Shaw FL, Harrison H, Spence K, Ablett MP, Simões BM, Farnie G, et al. A detailed mammosphere assay protocol for the quantification of breast stem cell activity. J Mammary Gland Biol Neoplasia. 2012;17(2):111-7. https://doi.org/10.1007/s10911-012-9255-3.
37. Wang Y, Chen X, Cao W, Shi Y. Plasticity of mesenchymal stem cells in immunomodulation: Pathological and therapeutic implications. Nat Immunol. 2014;15(11):1009-16. https://doi.org/10.1038/ni.3002.
38. Trickett A, Kwan YL. T cell stimulation and expansion using anti-cd3/cd28 beads. J Immunol Methods. 2003;275(1-2):251-5. https://doi.org/10.1016/s0022-1759(03)00010-3.
39.Paramita DA, H ermansyah D, P aramita DA, A malina ND. Regulation of p53 a nd survivin by C urcuma longa extract to caspase-3 dependent apoptosis in triple negative breast cancer cells. Medicinski Glasnik. 2022;19(2):189. https://doi: 10.17392/1453-22.
40. Rio DC, Ares M, Jr., Hannon GJ, Nilsen TW. Purification of rna using trizol (tri reagent). Cold Spring Harb Protoc. 2010;2010(6):pdb.prot5439. https://doi.org/10.1101/pdb.prot5439.
41. Kastenhuber ER, Lowe SW. Putting p53 in context. Cell. 2017;170(6):1062-78. https://doi.org/10.1016/j.cell.2017.08.028.
42. Livak KJ, Schmittgen TD. Analysis of relative gene expression data using real-time quantitative pcr and the 2(-delta delta c(t)) method. Methods. 2001;25(4):402-8. https://doi.org/10.1006/meth.2001.1262.
43. Vidal M, Cusick ME, Barabási AL. Interactome networks and human disease. Cell. 2011;144(6):986-98. https://doi.org/10.1016/j.cell.2011.02.016.
44. Ideker T, Krogan NJ. Differential network biology. Mol Syst Biol. 2012;8:565. https://doi.org/10.1038/msb.2011.99.
45. Luck K, Kim DK, Lambourne L, Spirohn K, Begg BE, Bian W, et al. A reference map of the human binary protein interactome. Nature. 2020;580(7803):402-8. https://doi.org/10.1038/s41586-020-2188-x.
46. Lane DP. Cancer. P53, guardian of the genome. Nature. 1992;358(6381):15-6. https://doi.org/10.1038/358015a0.
47. Kruiswijk F, Labuschagne CF, Vousden KH. P53 in survival, death and metabolic health: A lifeguard with a licence to kill. Nat Rev Mol Cell Biol. 2015;16(7):393-405. https://doi.org/10.1038/nrm4007.
48. Oren M, Rotter V. Mutant p53 gain-of-function in cancer. Cold Spring Harb Perspect Biol. 2010;2(2):a001107. https://doi.org/10.1101/cshperspect.a001107.
49. Liu Y, Burness ML, Martin-Trevino R, Guy J, Bai S, Harouaka R, et al. Rad51 mediates resistance of cancer stem cells to parp inhibition in triple-negative breast cancer. Clin Cancer Res. 2017;23(2):514-22. https://doi.org/10.1158/1078-0432.Ccr-15-1348.
50. Takaoka A, Hayakawa S, Yanai H, Stoiber D, Negishi H, Kikuchi H, et al. Integration of interferon-alpha/beta signalling to p53 responses in tumour suppression and antiviral defence. Nature. 2003;424(6948):516-23. https://doi.org/10.1038/nature01850.
51. Muñoz-Fontela C, Mandinova A, Aaronson SA, Lee SW. Emerging roles of p53 and other tumour-suppressor genes in immune regulation. Nat Rev Immunol. 2016;16(12):741-50. https://doi.org/10.1038/nri.2016.99.
52. Yang J, Nie J, Ma X, Wei Y, Peng Y, Wei X. Targeting pi3k in cancer: Mechanisms and advances in clinical trials. Mol Cancer. 2019;18(1):26. https://doi.org/10.1186/s12943-019-0954-x.
53. Korkaya H, Kim GI, Davis A, Malik F, Henry NL, Ithimakin S, et al. Activation of an il6 inflammatory loop mediates trastuzumab resistance in her2+ breast cancer by expanding the cancer stem cell population. Mol Cell. 2012;47(4):570-84. https://doi.org/10.1016/j.molcel.2012.06.014.
54. Prajoko YW, Heriyanto DS, Dirja BT, Susanto S, Lau V, Gunawan AN, et al. High frequency of the *PIK3CA* h1047l mutation in indonesian breast cancer across molecular subtypes. PLoS One. 2025;20(5):e0322154. https://doi.org/10.1371/journal.pone.0322154.
55. Zhang L, Yu D. Exosomes in cancer development, metastasis, and immunity. Biochim Biophys Acta Rev Cancer. 2019;1871(2):455-68. https://doi.org/10.1016/j.bbcan.2019.04.004.
56. Pegtel DM, Gould SJ. Exosomes. Annu Rev Biochem. 2019;88:487-514. https://doi.org/10.1146/annurev-biochem-013118-111902.
57. Hermansyah D, Paramita DA, Muhar AM, Amalina ND. Curcuma longa extract inhibits migration by reducing mmp-9 and rac-1 expression in highly metastatic breast cancer cells. Res Pharm Sci. 2024;19(2):157-66. https://doi.org/10.4103/rps.Rps_46_23.

58. Marotta LL, Almendro V, Marusyk A, Shipitsin M, Schemme J, Walker SR, et al. The jak2/*STAT3* signaling pathway is required for growth of cd44^{+}cd24^{-} stem cell-like breast cancer cells in human tumors. J Clin Invest. 2011;121(7):2723-35. https://doi.org/10.1172/jci44745.
59. Johnson DE, O'Keefe RA, Grandis JR. Targeting the il-6/jak/*STAT3* signalling axis in cancer. Nat Rev Clin Oncol. 2018;15(4):234-48. https://doi.org/10.1038/nrclinonc.2018.8.
60. Sharma P, Allison JP. Dissecting the mechanisms of immune checkpoint therapy. Nat Rev Immunol. 2020;20(2):75-6. https://doi.org/10.1038/s41577-020-0275-8.
61. Peng J, Hamanishi J, Matsumura N, Abiko K, Murat K, Baba T, et al. Chemotherapy induces programmed cell death-ligand 1 overexpression via the nuclear factor-κb to foster an immunosuppressive tumor microenvironment in ovarian cancer. Cancer Res. 2015;75(23):5034-45. https://doi.org/10.1158/0008-5472.Can-14-3098.
62. Voorwerk L, Slagter M, Horlings HM, Sikorska K, van de Vijver KK, de Maaker M, et al. Immune induction strategies in metastatic triple-negative breast cancer to enhance the sensitivity to *PD-1* blockade: The tonic trial. Nat Med. 2019;25(6):920-8. https://doi.org/10.1038/s41591-019-0432-4.
63. Hermansyah D, Syarifah S, Muhar AM, Putra A. Unveiling paclitaxel-induced mesenchymal stem cells: Orchestrating nrf2 modulation and apoptosis in cd44+/cd24- cancer stem cells. Breast Cancer (Dove Med Press). 2024;16:319-28. https://doi.org/10.2147/bctt.S457548.
64. DeNardo DG, Ruffell B. Macrophages as regulators of tumour immunity and immunotherapy. Nat Rev Immunol. 2019;19(6):369-82. https://doi.org/10.1038/s41577-019-0127-6.
65. Apetoh L, Ghiringhelli F, Tesniere A, Obeid M, Ortiz C, Criollo A, et al. Toll-like receptor 4-dependent contribution of the immune system to anticancer chemotherapy and radiotherapy. Nat Med. 2007;13(9):1050-9. https://doi.org/10.1038/nm1622.
66. Ghiringhelli F, Apetoh L, Tesniere A, Aymeric L, Ma Y, Ortiz C, et al. Activation of the nlrp3 inflammasome in dendritic cells induces il-1beta-dependent adaptive immunity against tumors. Nat Med. 2009;15(10):1170-8. https://doi.org/10.1038/nm.2028.
67. Zitvogel L, Galluzzi L, Smyth MJ, Kroemer G. Mechanism of action of conventional and targeted anticancer therapies: Reinstating immunosurveillance. Immunity. 2013;39(1):74-88. https://doi.org/10.1016/j.immuni.2013.06.014.
68. Galluzzi L, Buqué A, Kepp O, Zitvogel L, Kroemer G. Immunological effects of conventional chemotherapy and targeted anticancer agents. Cancer Cell. 2015;28(6):690-714. https://doi.org/10.1016/j.ccell.2015.10.012.
69. Denisenko TV, Budkevich IN, Zhivotovsky B. Cell death-based treatment of lung adenocarcinoma. Cell Death Dis. 2018;9(2):117. https://doi.org/10.1038/s41419-017-0063-y.
70. André F, Ciruelos E, Rubovszky G, Campone M, Loibl S, Rugo HS, et al. Alpelisib for *PIK3CA*-mutated, hormone receptor-positive advanced breast cancer. N Engl J Med. 2019;380(20):1929-40. https://doi.org/10.1056/NEJMoa1813904.
71. Jones RH, Casbard A, Carucci M, Cox C, Butler R, Alchami F, et al. Fulvestrant plus capivasertib versus placebo after relapse or progression on an aromatase inhibitor in metastatic, oestrogen receptor-positive breast cancer (faktion): A multicentre, randomised, controlled, phase 2 trial. Lancet Oncol. 2020;21(3):345-57. https://doi.org/10.1016/s1470-2045(19)30817-4.
72. Bendell JC, Earle M, Hosein PJ, Seetharam M, Sharma S, Bullock AJ, et al. A phase 3 randomized, double-blind, placebo-controlled study of napabucasin (bbi-608) in combination with gemcitabine and nab-paclitaxel versus gemcitabine and nab-paclitaxel alone in patients with metastatic pancreatic adenocarcinoma (canstem111p). J clin oncol. 2019;37(15_suppl):4005.
73. Hong D, Kurzrock R, Kim Y, Woessner R, Younes A, Nemunaitis J, et al. Azd9150, a next-generation antisense oligonucleotide inhibitor of *STAT3* with early evidence of clinical activity in lymphoma and lung cancer. Sci Transl Med. 2015;7(314):314ra185. https://doi.org/10.1126/scitranslmed.aac5272.